

# Simulations of CALIPSO Lidar Data

Kathleen A. Powell<sup>a</sup>, Willam H. Hunt<sup>b</sup>, David M. Winker<sup>c</sup>

<sup>a</sup>Science Applications International Corporation

<sup>b</sup>Wyle Laboratories

<sup>c</sup>NASA Langley Research Center

NASA Langley Research Center, Mail Stop 435, Hampton, VA 23681

Tel: 757-864-2688 Fax: 757-864-7775, Email: [k.a.powell@larc.nasa.gov](mailto:k.a.powell@larc.nasa.gov)

## ABSTRACT

Simulated CALIPSO lidar data are required to test the CALIPSO lidar level 1 and level 2 algorithms. A simulator program has been developed to simulate the expected instrument performance for a range of atmospheric conditions and generate simulated data that can be used to predict instrument performance during operations, compare with instrument test results, and serve as a realistic test bed for algorithm development.

## 1. INTRODUCTION

The CALIPSO mission, to be launched in April 2004, will obtain global aerosol and cloud measurements from space<sup>1</sup>. These measurements will provide improved observations of aerosols and clouds needed for use in global climate models. CALIPSO consists of three co-aligned, near-nadir viewing instruments: a 2-wavelength polarization-sensitive lidar, an imaging infrared radiometer (IIR), and a high-resolution wide field camera.

Currently in development are algorithms to produce calibrated and geolocated level 1 data products for each instrument and to derive geophysical variables for the IIR and lidar level 2 data products. Testing the functionality of these algorithms requires high-fidelity simulated data. A software simulation of the CALIPSO lidar has been developed to produce simulated lidar backscatter profiles for this purpose. This tool generates simulated data that matches the expected performance of the CALIPSO lidar, including its random noise characteristics. The simulation was developed in a modular approach and is easily updated as the lidar instrument design matures. It also has the flexibility to produce a wide range of simulated data because it can accept an unlimited combination of atmospheric and instrument parameter settings. By adjusting the instrument parameter settings, the simulated data can be made to match the expected performance of the actual instrument at any stage in its lifetime. Output simulated data includes 1064 nm total backscatter profiles and 532 nm backscatter profiles for both the parallel and perpendicular polarization states.

## 2. SIMULATED LIDAR DATA

Simulated lidar data are currently being used to test the performance of the CALIPSO lidar level 1 and level 2 algorithms. These include algorithms for instrument calibration (level 1) and the retrieval of spatial and optical characteristics of clouds and aerosol layers (level 2). Because they are applied to a broad range of atmospheric targets, each of these algorithms has different requirements for test data. To produce the appropriate simulated data for testing, the CALIPSO lidar simulator enables the user to define multiple aerosol and cloud layers with varying optical properties to represent the types of lidar measurements that will be encountered in the actual lidar data. The simulated data may be simple such as a simulation of clear sky conditions, or a complex simulation containing multiple embedded aerosol and cloud layers.

An example of simulated lidar data for six individual scenes for the 532 nm parallel channel is shown in Figure 1. To generate these simulated data, layer descriptors for each of the scenes were input into the simulator. Six attenuated backscatter profiles were built in the atmospheric module according to the layer specifications and each profile was run

through the instrument module 1500 times to produce a block of simulated data. Table 1 lists the layer descriptions for each scene as defined for the 532 nm input and includes the profile number, layer description, base and top altitude (km), volume-extinction coefficient ( $\sigma$ ,  $\text{km}^{-1}$ ), extinction-to-backscatter ratio ( $S$ ), and depolarization ratio ( $\delta$ ). The scenes were defined to contain single, multiple, and embedded layers with varying optical properties.

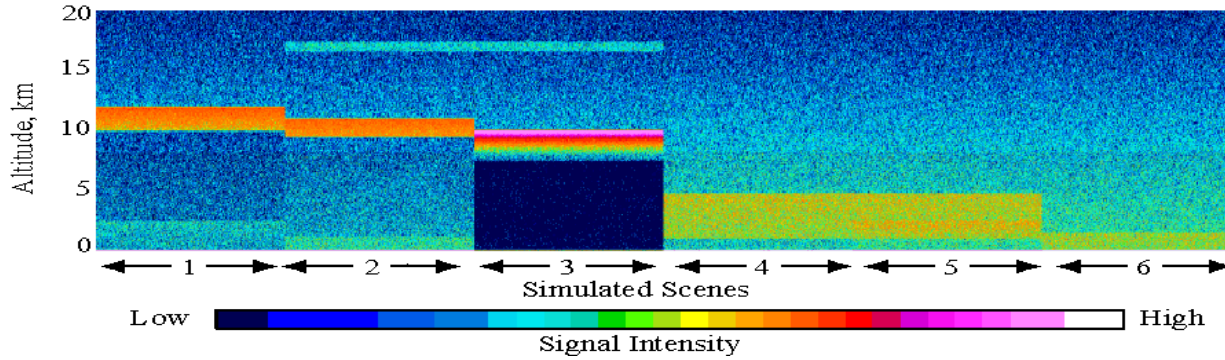


Fig. 1 Intensity plot of simulated 532 nm parallel channel lidar backscatter profiles for six input profiles. 1500 simulated profiles were generated for each input profile. The color assigned to each pixel represents the intensity of the signal.

Table 1. Layer descriptions for the six profiles input into the simulator to produce the example image in Figure 1.

Scene	Type	Layer, km	$\sigma$ , $\text{km}^{-1}$	$S$	$\delta$	Scene	Type	Layer, km	$\sigma$ , $\text{km}^{-1}$	$S$	$\delta$
1	Cirrus	10-12	0.25	25.0	0.4	3	Cirrus	16.6-17.4	0.025	30.0	0.5
1	Aerosol	0-2.5	0.08	60.9	0.0	3	Cirrus	7.5-10	1.0	15.0	0.4
						3	Aerosol	0-1.2	0.05	40.289	0.1
2	Cirrus	16.6-17.4	0.025	30.0	0.5						
2	Cirrus	9.5-11	0.2	22.5	0.4	5	Aerosol	0-2.5	0.08	60.9	0.0
2	Aerosol	0-1.2	0.05	40.789	0.1	5	Aerosol	1-4.8	0.045	21.979	0.01
4	Aerosol	1-4.8	0.045	21.979	0.01	6	Aerosol	0-1.5	0.05	40.289	0.1

### 3. ATMOSPHERIC AND INSTRUMENT MODULES

The atmospheric module builds the model atmosphere for the simulator in the form of 532 nm parallel and perpendicular and 1064 nm CALIPSO attenuated backscatter  $\beta(r)T^2(r)$  profiles, where  $r$  is the range from the receiver.  $\beta(r)$  is the composite volume-scattering coefficient formed by summing the altitude dependent molecular, aerosol, and cloud volume-scattering coefficients.  $T^2(r)$  is the two-way transmission between the lidar and the sample volume,

$$T^2(r) = e^{-2 \int_0^r \sigma(r') dr'} \quad (1)$$

where  $\sigma(r')$  is the composite volume-extinction coefficient formed by summing the altitude dependent molecular, aerosol, and cloud volume-extinction coefficients. Background radiances are also supplied and computed by a two-stream, plane parallel model, which computes a top of the atmosphere radiance from single Rayleigh scattering plus a Lambertian surface and overlying layer. The user has the option to define the optical and spatial properties of the molecular, aerosol, and cloud components for each profile in the atmosphere model or provide attenuated backscatter profiles from existing lidar measurements such as LITE<sup>2</sup> and SOLVE<sup>3</sup>. The user defined option requires the user to select a density profile and define the aerosol and cloud layer optical properties and descriptors. Layers may be overlapping, contiguous, or separated. Layer descriptions include base and top heights and a shape factor which varies from rectangular to curved. The layer optical properties include wavelength dependent volume-scattering and volume-extinction coefficients and depolarization ratio for 532 nm. In addition to the layer definitions, the user must also specify the lighting conditions, surface wind speed, surface albedo, and solar zenith angle. Currently, the user defined model only includes single scattering and methods to incorporate multiple scattering are being studied and will be included in the near future. The atmosphere model input into the instrument module may be processed as a single profile multiple times or as a multiple

of profiles one at a time. For either case, one profile at a time is input into the instrument module and the effects of the instrument are applied at each range bin.

The instrument module closely models the expected performance of the CALIPSO lidar. The specifications and functions of the instrument components are obtained from vendor specification tables, tests of individual lidar components, and conversations with engineers developing and testing the lidar. The instrument module description in this paper is divided into subsystems that function identically for 532 nm and 1064 nm, unless otherwise specified.

The satellite subsystem defines the spacecraft altitude and off-nadir angle, which are used to determine range from the spacecraft to the Earth and to the lidar measurements.

The laser transmitter subsystem parameters: transmitted laser energy, effective transmitter beam divergence, laser pulse length, and laser pulse width are input into the receiver optics module to compute the received power backscattered from the atmospheric particles. The transmitted laser energy is a function of both the laser pulse energy and the optical efficiency of the beam expander, and the effective transmitter beam divergence is a function of both the transmitted beam divergence and telescope blur circle.

The receiver subsystem simulates the performance of the receiver telescope, optical filters, and detectors. The amount of light collected by the telescope depends upon the primary mirror effective area (after taking obscurations into account). The fraction of the light that gets through the receiver and on to the detectors is determined by the transmission of the field stop that determines the field-of-view, the throughputs (reflectivity or transmission) of the optical elements in the receiver, and the optical filter transmissions. Included in the calculation of the field stop transmission for the backscatter energy are the effective transmitter beam divergence, the receiver field-of-view, the separation of the laser and telescope axes, and the boresight misalignment angle. The field stop transmission for the solar background is determined by the receiver field-of-view.

For the optical filters, the optical throughput is treated differently for backscatter and for background. To compute the fraction of the backscatter energy that is transmitted through the filter, the product of the normalized laser energy and the filter transmission is integrated over a range of wavelengths centered on the laser center wavelength. The laser spectral energy distribution is assumed to be Gaussian. The transmission curve for 532 channel Fabry-Perot etalon is modeled as an Airy function<sup>4</sup>, and manufacturer-provided curves are used for the interference filters for both wavelengths. The throughput for solar background light is determined by the area under the transmission curve of the interference filter for the 1064 channel, or the combined etalon and blocking filter for the 532 channels.

When the return signal reaches the detector, the number of photons per second  $N(r)$  collected by the receiver from a volume of atmosphere at specified range  $r$ ,

$$N(r) = N_{Bks}(r) + N_{Bkg} \quad (2)$$

is the sum of  $N_{Bks}(r)$ , the number of photons per second backscattered from a volume of atmosphere at a specified range  $r$ , and  $N_{Bkg}$ , the number of photons due to background radiation. Equations for these terms can be written as

$$N_{Bks}(r) = \beta(r)T^2(r)kE_0 \frac{\lambda_0}{hc} \frac{1}{\tau_L} \frac{c\tau_L}{2} \frac{mA}{r^2} T_{OF} T(r)_{ABks} T_{FBks}, \quad (3)$$

$$N_{Bkg} = L_S \frac{\lambda_0}{hc} \frac{mA}{r^2} T_{OF} T_{ABkg} T_{FBkg}. \quad (4)$$

In Eqs. (2)-(4),  $\beta(r)T^2(r)$  is the attenuated backscatter coefficient,  $k$  is the optical efficiency of the lidar transmitter,  $E_0$  is laser pulse energy,  $\lambda_0$  is the wavelength,  $h$  is Planck's constant,  $c$  is speed of light,  $\tau_L$  is pulse length,  $m$  is the fraction of primary mirror area not obscured,  $A$  is area of the receiver at the primary mirror,  $L_S$  is background radiance,  $T_{OF}$  is overall optical transmission, excluding field stop transmission and blocking/etalon or interference filters,  $T(r)_{ABks}$  and  $T_{ABkg}$  are field stop transmissions for backscatter and background light, respectively, and  $T_{FBks}$  and  $T_{FBkg}$  are the blocking/etalon or interference filter transmission factors for backscatter and background light, respectively.

Two detector models are defined in the simulator. One simulates the photomultiplier tube (PMT) for the 532 nm parallel and perpendicular channels, and the other simulates the 1064 nm avalanche photodiode (APD). For both models, the electron generation at the PMT and APD photocathode depends upon photon arrival rate, the detector quantum efficiency, and detector dark count rate. The photon arrival rate is a random process and is simulated by Poisson statistics. The number of photoelectrons per 0.1  $\mu$ sec  $\phi_E(r)$  generated at the photocathode from a volume of atmosphere at specified range  $r$  is obtained as

$$\phi_E(r) = P_p(\phi | (N(r)\eta_q + N_D) \cdot 0.1\mu\text{sec}) \quad (5)$$

where  $P_p(\phi | (N(r)\eta_q + N_D) \cdot 0.1\mu\text{sec})$  represents the Poisson deviate function. This function is used to determine the probability of generating  $\phi$  photoelectrons at the photocathode with the mean arrival rate of  $(N(r)\eta_q + N_D)$  photoelectrons per 0.1  $\mu$ sec. Defining the unit time for photoelectron generation at 0.1  $\mu$ sec models the lidar sampling frequency,  $\eta_q$  is the detector quantum efficiency, and  $N_D$  is the detector dark counts per second.

The detector gain is also simulated by a random process and is defined for each detector model. The statistical spread of secondary electron emissions for the PMT is represented in the simulation by cascading Poisson distributions at each dynode. Noise in the avalanche process of the APD is based on a model, developed by McIntyre<sup>5</sup>, that considers the statistical nature of avalanche multiplication. Multiplication by elemental electron charge results in a gain amplified signal current at the anode in amperes for each 0.1  $\mu$ sec range bin.

The post-amplification and filtering subsystem simulates the functions of the transimpedance amplifier (TIA), post-amplifiers, post-filter, and analog-to-digital converter. To simulate the electronic background subtraction function of the TIA, the average background value is computed and subtracted prior to subsequent processing. The background-subtracted signal is multiplied by a constant gain factor in volts/ampere to produce a signal in volts, and post-amplifiers provide additional voltage amplification to the signal according to day or night conditions. A dc offset is also added at this point. To simulate the post-filter, which temporally spreads and combines the effects of each signal pulse, the signal is convolved with the system impulse response function. To simulate the analog-to-digital conversion, the convolved analog signal is multiplied by a conversion factor to convert from volts to digitizer reading.

The data handling subsystem simulates the payload data handling system, which performs the on-board averaging and packaging of the downlink data. Before the backscatter profiles are averaged, a baseline value is computed from a high altitude region and subtracted from the return signal. On-board averaging is then performed to reduce the size of the downlink data. The simulated digitized 1064 nm total backscatter signals and 532 nm backscatter signals for both the parallel and perpendicular polarization states are vertically and horizontally averaged at various resolutions within specified altitude regions and stored as a major frame data.

#### 4. SUMMARY

A software simulation of the CALIPSO lidar has been developed to generate 1064 nm total backscatter profiles and 532 nm backscatter profiles for both the parallel and perpendicular polarization states. This simulation will be updated as actual test data are available. Data from this simulation are currently used for testing the CALIPSO lidar level 1 and level 2 algorithms. The simulation will also be used to predict the degradation of the instrument performance with age.

#### REFERENCES

1. D. M. Winker, "The CALIPSO Mission", current proceedings (2002).
2. D. M. Winker, R. H. Couch, and M. P. McCormick, "An overview of LITE: NASA's lidar in-space technology experiment," Proceedings of the IEEE, Vol. 84, No. 2, February, 1996.
3. C. A. Hostetler, The SAGE III Ozone Loss and Validation Experiment (SOLVE), November 1999-March 2000 (private communication).
4. P. D. Atherton, N. K. Reay, J. Ring, T. R. Hicks, "Tunable Fabry-Perot filters," Optical Engineering, Vol. 20 No. 6, pp. 806-814, November/December 1981.
5. P. P. Webb, R. J. McIntyre, and J. Conradi, "Properties of Avalanche Photodiodes." RCA Review, Vol.35, June, 1974.